

**Size dependence of carrier dynamics and carrier multiplication in PbS quantum dots**Gero Nootz,<sup>1,2</sup> Lazaro A. Padilha,<sup>1</sup> Larissa Levina,<sup>3</sup> Vlad Sukhovatkin,<sup>3</sup> Scott Webster,<sup>1</sup> Lukasz Brzozowski,<sup>3</sup> Edward H. Sargent,<sup>3</sup> David J. Hagan,<sup>1,2,\*</sup> and Eric W. Van Stryland<sup>1,2,†</sup><sup>1</sup>CREOL: The College of Optics and Photonics, University of Central Florida, 4000 Central Florida Blvd., Orlando, Florida, 32816, USA<sup>2</sup>Physics Department, University of Central Florida, 4000 Central Florida Blvd., Orlando, Florida, 32816, USA<sup>3</sup>The Edward S. Rogers Sr. Department of Electrical and Computer Engineering, University of Toronto, Toronto, Ontario, Canada, M5S3G4

(Received 26 October 2010; revised manuscript received 17 February 2011; published 5 April 2011)

The time dynamics of the photoexcited carriers and carrier-multiplication efficiencies in PbS quantum dots (QDs) are investigated. In particular, we report on the carrier dynamics, including carrier multiplication, as a function of QD size and compare them to the bulk value. We show that the intraband  $1P \rightarrow 1S$  decay becomes faster for smaller QDs, in agreement with the absence of a phonon bottleneck. Furthermore, as the size of the QDs decreases, the energy threshold for carrier multiplication shifts from the bulk value to higher energies. However, the energy threshold shift is smaller than the band-gap shift and, therefore, for the smallest QDs, the threshold approaches  $2.35 E_g$ , which is close to the theoretical energy conservation limit of twice the band gap. We also show that the carrier-multiplication energy efficiency increases with decreasing QD size. By comparing to theoretical models, our results suggest that impact ionization is sufficient to explain carrier multiplication in QDs.

DOI: [10.1103/PhysRevB.83.155302](https://doi.org/10.1103/PhysRevB.83.155302)

PACS number(s): 73.21.La, 78.67.Hc

**I. INTRODUCTION**

Multiexciton generation (MEG) or carrier multiplication (CM) is a process in which more than one electron-hole pair is created as the result of the absorption of a single photon. This process, which in bulk semiconductors is explained by impact ionization,<sup>1-3</sup> is one possible channel of relaxation for highly excited carriers. It is expected to be stronger in semiconductor quantum dots (QDs) due to the stronger carrier-carrier interaction and the lack of a well-defined translational momentum in the spatially localized quantum-confined levels. This, in turn, could potentially contribute to the realization of more efficient photovoltaic devices.<sup>4-6</sup> In the ideal case, the threshold for CM determined by energy conservation is  $2 E_g$  (here,  $E_g$  is the energy of the  $1S_h \rightarrow 1S_e$  transition in QDs, which we refer to as the band gap),<sup>6</sup> and the electron-hole-pair creation energy  $\varepsilon$ , defined as energy above the CM threshold required to create an additional electron-hole pair, is  $1 E_g$ .<sup>7</sup>

Considerable excitement has been created over the possibility of enhancing CM in semiconductor QDs and its potential implications on highly efficient solar energy conversion. Nevertheless, many questions concerning this effect remain unanswered. Some early reports showed extremely high CM efficiency in several different species of QDs.<sup>8-12</sup> Recent publications<sup>13,14</sup> show that this extremely high CM efficiency in QDs is misleading. Furthermore, the physical mechanism of CM in QDs remains under debate.<sup>1,2,7,14-19</sup> Some reports suggest that direct generation of a biexciton from the strong Coulomb interaction of the quantum-confined carriers through exciton<sup>1</sup> or biexciton<sup>7</sup> virtual levels needs to be invoked to explain the high efficiency of CM in QDs. Others propose that, as for the case of bulk semiconductors, impact ionization can explain the effect without invoking quantum-confinement effects.<sup>15,19,20</sup>

To answer these questions on QDs, it is necessary to study the temporal dynamics of the photoexcited carriers in such structures. Despite extensive theoretical and experimental investigations of carrier dynamics and CM in QD

structures,<sup>1,2,7,14-19</sup> especially PbSe, there is little work done on PbS, a material that exhibits a more symmetric and isotropic band structure. Here, we perform a systematic study of the influence of QD size on carrier dynamics and CM efficiency in PbS QDs, the band gap of which ranges from 0.63 to 1.34 eV. We perform CM measurements at different pump photon energies to investigate how the CM threshold and electron-hole-pair creation energy depend on the size of the PbS QDs. We show that the intraband  $1P \rightarrow 1S$  decay occurs on a picosecond to subpicosecond time scale and is faster for smaller QDs. This follows the same trend observed in PbSe (Ref. 21) and CdSe (Ref. 22) QDs and confirms the absence of the phonon bottleneck. We compare our results to a recently published study of CM in bulk PbS.<sup>2</sup> We observe a clear dependence of the carrier-multiplication energy threshold  $\hbar\omega_{th}$  and the electron-hole-pair creation energy  $\varepsilon$ , on the QD size. The results show that the efficiency of transfer of photon energy to the carrier-multiplication process is increased in smaller QDs compared to bulk PbS.

The samples investigated here are PbS colloidal quantum dots that are capped using oleic acid and suspended in toluene. It has previously been reported<sup>23</sup> that such quantum dots are well passivated in as much as they exhibit high photoluminescence quantum yields (as high as 80%), suggesting a minimum of deep traps and/or midgap recombination centers. The QDs are grown using a solution-based organometallic route.<sup>24</sup> In brief, the QDs were synthesized and purified using standard air-free techniques in a two-neck flask equipped with magnetic stirrer, thermocouple, and heating mantle. Lead oleate stock solution used for PbS synthesis was prepared by pumping the mixture of 4.0 mmol of PbO (0.9 g), 9.5 mmol (2.67 g) of oleic acid (OA), and 18.8 mmol (4.73 g) of 1-octadecene (ODE) at 100 °C for 16 hours. The sulfur precursor was prepared in a nitrogen-filled glove box by mixing bis(trimethylsilyl) sulfide (TMS) with ODE. The size of the quantum dots was controlled by varying the injection temperature and TMS concentration.

The PbS QDs are prepared in 1-mm quartz cells with optical density (OD) lower than 0.1 (typically  $\sim 0.05$ ) at the  $1S_h \rightarrow 1S_e$  peak. This is done to avoid strong depletion of the excitation beam at photon energies far above  $E_g$ , where the optical densities tend to be large. The QD's one-photon absorption spectra are measured using a Cary-500 spectrophotometer and the cross sections are calculated from the empirical method proposed by Cademartiri *et al.*<sup>25</sup> using the optical density integrated under the low-energy side of the  $1S_h \rightarrow 1S_e$  peak. Herein we refer to QD samples based on the wavelength of the  $1S_h \rightarrow 1S_e$  peak, e.g., the sample with the  $1S_h \rightarrow 1S_e$  peak at 1140 nm is named PbS-1140.

We investigate the dynamics of photoexcited carriers, and of CM, via transient absorption in pump-probe experiments. The samples are excited with femtosecond pulses (130–170 fs, FWHM) from two optical parametric generators and amplifiers (OPG/OPA TOPAS-800, Light Conversion), with wavelength ranging from 300 to 2600 nm. Each OPG/OPA is pumped using a chirped-pulse amplified Ti:sapphire laser system (CPA-2010, Clark-MXR) operating at 1 kHz and delivering 140-fs (FWHM), 1.7-mJ pulses at 780 nm. Pump and probe beams overlap in the sample at a small angle ( $<5^\circ$ ). The pump beam is selected from one OPA, while the second OPA is set at 1300 nm and used to generate a white-light continuum (WLC) in a 3-mm thick  $\text{CaF}_2$  crystal. The probe wavelength is selected from the WLC using  $\sim 10$ -nm bandpass filters.<sup>26</sup> The transmitted probe beam is detected with home-built Si and Ge photodiode detectors for wavelengths up to 1.7  $\mu\text{m}$  and Thorlabs PDA30G PbS detectors for longer-wavelength measurements up to 2.9  $\mu\text{m}$ . Narrow bandpass filters ( $\sim 10$  nm bandwidth) are used in front of the detectors to avoid the influence of scattered pump light and QD photoluminescence.

### A. Carrier dynamics

To investigate the carrier dynamics, we excited the QDs at energies slightly above the  $1P_h \rightarrow 1P_e$  transition and probed them using different photon energies ranging from the  $1P_h \rightarrow 1P_e$  to the  $1S_h \rightarrow 1S_e$  transition. Figure 1 illustrates the change in absorption ( $\Delta\alpha$ ) for a sample of PbS QDs with band gap at 1220 nm at different time delays after the sample has been excited by the pump. Also shown are the linear absorption spectra and second derivative thereof. The temporal evolution of the photoexcited carriers shown in Fig. 1 indicates that, once excited, the carriers decay from the  $1P$  state to the  $1S$  level with intraband relaxation time of less than 1 ps (this is shown by the decrease of the third peak and increase of the first peak of the transient absorption). The size dependence of the  $1P \rightarrow 1S$  decay is shown in Figs. 2(a) and 2(b). From the  $1S$  state, the carriers recombine either via radiative decay or Auger recombination [Fig. 2(c)]. The biexciton Auger lifetime varies by one order of magnitude, ranging from 10 to 200 ps for the size range studied. The peaks observed in the transient absorption experiment (marked 1–3 in Fig. 1) correspond to the positions of the one-photon transitions as indicated by the valleys of the second derivative of the linear absorption. The increase in absorption between the  $1P_h \rightarrow 1P_e$  and  $1S_h \rightarrow 1S_e$  transitions is due to the redshift of the absorption spectra caused by Coulomb interaction between the photoexcited carriers.<sup>27,28</sup> A weak feature between

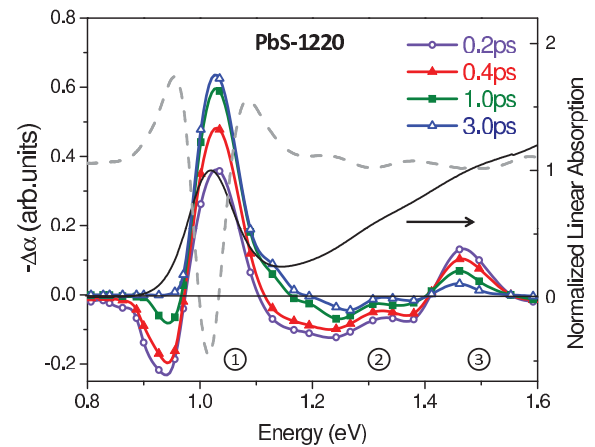


FIG. 1. (Color online) Change in the linear absorption of PbS QDs due to photoexcitation at different time delay after the excitation pulse. The excitation is at 750 nm (1.66 eV). The black continuous line is the linear absorption and the gray dashed line is the second derivative of the linear absorption. The three peaks identified in the second derivative and in the spectral dynamics correspond to (1)  $1S_h \rightarrow 1S_e$ , (2)  $1S_h \rightarrow 1P_e$  and  $1P_h \rightarrow 1S_e$ , and (3)  $1P_h \rightarrow 1P_e$ .

the  $1P_h \rightarrow 1P_e$  and  $1S_h \rightarrow 1S_e$  transitions (marked as feature 2 in Fig. 1, and also seen in the second derivative) is attributed to the formally parity-forbidden  $1P_h \rightarrow 1S_e$  and  $1S_h \rightarrow 1P_e$  transitions, which have been shown to become increasingly allowed in smaller lead-salt QDs.<sup>29</sup>

The temporal evolution of the depletion of the  $1P_h \rightarrow 1P_e$  and  $1S_h \rightarrow 1S_e$  transition is shown in Figs. 2(a) and 2(b) as a function of the QD size. As previously observed in other QD materials,<sup>21,22</sup> for PbS QDs, the  $1P \rightarrow 1S$  intraband decay becomes faster as the QD radius decreases [Fig. 2(a)], demonstrating the absence of the phonon bottleneck. In Fig. 2(b), we compare the energy loss rate, defined as the ratio between the  $1P \rightarrow 1S$  energy and the decay lifetime for different sizes of PbS QDs, with similar sizes of PbSe QDs from Ref. 21. For a given QD radius, both materials have similar energy loss rates. For CdSe QDs, the fast intraband decay is due to an Auger-type recombination,<sup>22</sup> and in PbS and PbSe QDs,<sup>21</sup> the high symmetry between the conduction and valence bands makes the probability of Auger-type intraband decay negligible. In these lead-salt QDs, the mechanism responsible for the fast intraband decay is still under debate,<sup>21,30,31</sup> therefore, it has been tentatively explained by multiphonon emission,<sup>21,31</sup> as previously demonstrated for PbSe QDs.<sup>21</sup> The lifetime of the ultrafast  $1P \rightarrow 1S$  decay observed here is shorter than previously reported by Istrate *et al.*<sup>32</sup> in PbS QDs with the  $1S_h \rightarrow 1S_e$  transition at 1550 nm. (We measured  $\sim 900$  fs, while the reported value in Ref. 32 is  $\sim 4$  ps.) The difference is probably explained by the longer pulse width used in Ref. 32 (2 ps), so the measured  $1P \rightarrow 1S$  decay could have been limited by the temporal resolution of the experiment.

Figure 2(c) shows the depletion of the  $1S$  level as a function of the average number of absorbed photons per QD for a sample with a band gap at 1500 nm. No further depletion of the linear absorption is observed for excitations higher than approximately eight photons per QD, generating an average of approximately eight electron-hole pairs per QD (the number is not exactly eight due to the small depletion of the pump

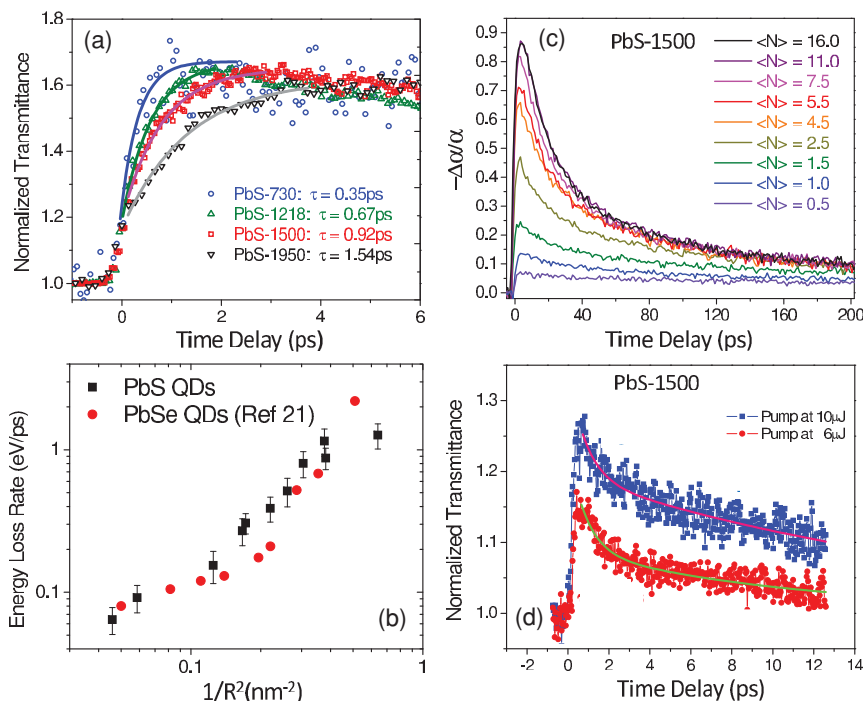


FIG. 2. (Color online) (a)  $1P \rightarrow 1S$  decay for different sizes of PbS QDs. (b) Energy loss rate for the intraband  $1P$ - $1S$  vs the inverse square of the QD radii showing the size dependence for PbS QDs compared to the same for PbSe QDs from Ref. 21. (c) The normalized change in absorption vs time delay shows the depletion of the  $1S$  state at several different pump fluences. The pump is at 870 nm and the probe at 1500 nm ( $1S_h \rightarrow 1S_e$ ). (d) Normalized transmittance vs time delay pumped at 870 nm and probed at 1064 nm ( $1P_h \rightarrow 1P_e$ ), showing the  $1P$  state depopulation at high pump fluences (more than eight photons absorbed per QD on average). The magnitude of the long-lived process increases for higher pump fluence, while the lifetimes for the fast decay (900 fs) and the slow decay (12 ps) remain the same for both pump fluences.

beam through the sample, which has an optical density  $\sim 0.1$  at the pump wavelength of 870 nm. For such high excitations, the long delay signal (after the multiexcitons have decayed via interband Auger recombination) is  $\sim 1/8$  of the peak change in transmittance at zero delay, suggesting that the  $1S$  level is eight-fold degenerate as previously demonstrated.<sup>32</sup> For higher excitation, no additional change occurs in the dynamics of the  $1S$  level; however, for the  $1P$  state, a long-lived decay ( $\sim 10$  ps) is observed [Fig. 2(d)] for excitations larger than eight photons per QD. If the excitation level is increased further, the only difference observed is an increase in the magnitude of the long-lived process, showing that, independent of the number of photoexcited carriers in PbS QDs, only eight carriers can decay to the  $1S$  level [Fig. 2(d)]. Due to the relatively fast interband Auger recombination of multiexcitons in the  $1S$  state, one could argue that the slow component of the intraband  $1P$  decay is due to a repopulation of the  $1S$  level after this state loses electrons via Auger recombination. However, the absence of significant changes in the  $1S$  dynamics at higher excitation [see the two highest excitations shown in Fig. 2(c)] rules out this possibility,<sup>32</sup> indicating either an influence of trap states, directly from the  $1P$  level<sup>33</sup> or direct  $1P_e \rightarrow 1P_h$  recombination. In well-passivated CdSe/ZnSe core-shell structures, it has been shown that, after saturating the population of the  $1S$  level, carriers at the  $1P$  level tend to recombine through direct  $1P_e \rightarrow 1P_h$  radiative decay.<sup>34</sup> In steady-state photoluminescence experiments on PbS QDs, no

direct  $1P_e \rightarrow 1P_h$  radiative recombination has been observed; however, due to the short lifetime ( $\sim 10$  ps), time-resolved photoluminescence experiments would be necessary to verify the presence of this decay channel.

## B. Carrier multiplication

Figure 3 shows the spectral behavior of the CM quantum efficiency, defined by the number of electron-hole pairs per absorbed photon, for five different sizes of PbS QDs with band gaps ranging from 0.63 to 1.34 eV, and for bulk PbS as measured in Ref. 2. The carrier multiplication is studied by monitoring the transient absorption at the  $1S_h \rightarrow 1S_e$  transition as the pump photon energies are varied. The presence of multiexcitons in the  $1S$  levels under low pump fluence allows the CM threshold and electron-hole-pair creation energies to be determined. For wavelengths where CM is expected, the pump-probe experiments are performed at several different pump fluences for which the average maximum number of absorbed photons per QD is less than 0.2. This is done to reduce the probability that more than one photon is absorbed per QD.

The magnitude of the CM efficiency is obtained from the fitting of the  $A/B$  ratio ( $A$  is the change in transmittance at zero delay and  $B$  is the change in transmittance for delay longer than the Auger recombination lifetime) for the lowest fluences and extrapolated to the limit for zero fluence. For

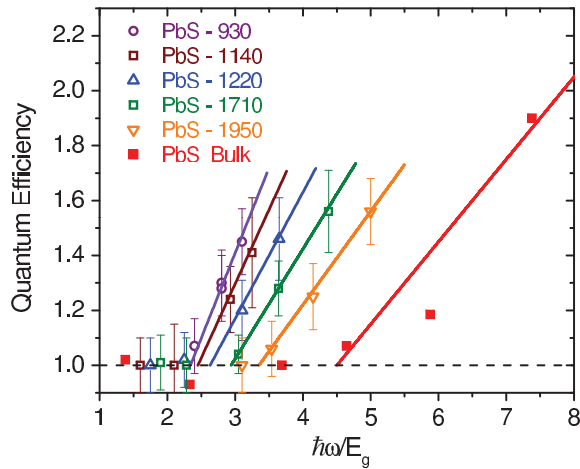


FIG. 3. (Color online) Spectral dependence of the carrier multiplication for five different sizes of PbS QDs compared to bulk PbS. The data for bulk PbS are from Ref. 2.

each QD in Fig. 3, the CM efficiency is fit with a straight line. The inverse of the slope defines the electron-hole-pair creation energy  $\varepsilon$ , and the CM energy threshold ( $\hbar\omega_{th}$ ) is defined by the point where the fit intersects the line  $CM = 1$ . From the fits in Fig. 3, we extract that  $\hbar\omega_{th}$  continuously decreases from  $4.5 E_g$  for bulk PbS to  $2.35 E_g$  for the smallest QDs as shown in Fig. 4(a). Note that, if plotted in eV (in terms of absolute energy instead of the QD band gap) as shown in Fig. 4(b),  $\hbar\omega_{th}$  is approximately constant at  $\sim 2.1$  eV for the two largest QDs as well as for bulk PbS, and increases only for QDs with

$E_g > 1$  eV. Figures 4(c) and 4(d) also show the dependence of  $\varepsilon$  on the QD size, i.e., it decreases from  $3.4 E_g$  in bulk PbS down to  $1.7 E_g$  for the smallest QD (PbS-930). These size-dependent results show that the CM efficiency at a given photon energy is larger for larger QDs and ultimately it tends to match that for bulk PbS; however, the energy efficiency, i.e., the amount of photon energy transferred to the creation of additional electron-hole pairs increases as the QD size decreases. In bulk semiconductors,  $\varepsilon$  far exceeds the energy-conservation limit of  $\varepsilon = E_g$  due to the translational momentum conservation requirements. The influence of the relaxation of conservation of translational momentum on the CM efficiency in QDs is still an object of controversy.<sup>12,12,20</sup> Yet, the lower limit of  $\varepsilon$  achieved for smaller QDs, as shown in Fig. 4(c), suggests that the relaxation of the translational momentum conservation requirements due to the highly localized wave functions plays a role in determining  $\varepsilon$ .<sup>12,14</sup> These results are in line with recent findings by Beard *et al.*<sup>12</sup> for colloidal PbSe QDs and Sambur *et al.*<sup>35</sup> for PbS QDs films. Our results reinforce the conclusions from Ref. 12 and add that  $\varepsilon$  is size dependent, being smaller, in terms of  $E_g$  normalized energy, for smaller QD [see Fig. 4(c)].

To the best of our knowledge, no definitive theoretical study of CM in PbS QDs is available. Nevertheless, several authors have reported on the possible mechanisms involved in CM in other QD structures, including PbSe QDs.<sup>1,7,15,19,20</sup> Theoretical predictions from Luo *et al.*<sup>18</sup> suggest that the most important aspects defining the CM efficiency and threshold in QDs are the materials density of states and the degeneracy of the  $1S_e$  state. For PbS and PbSe, the  $1S_e$  state is eight-fold degenerate.

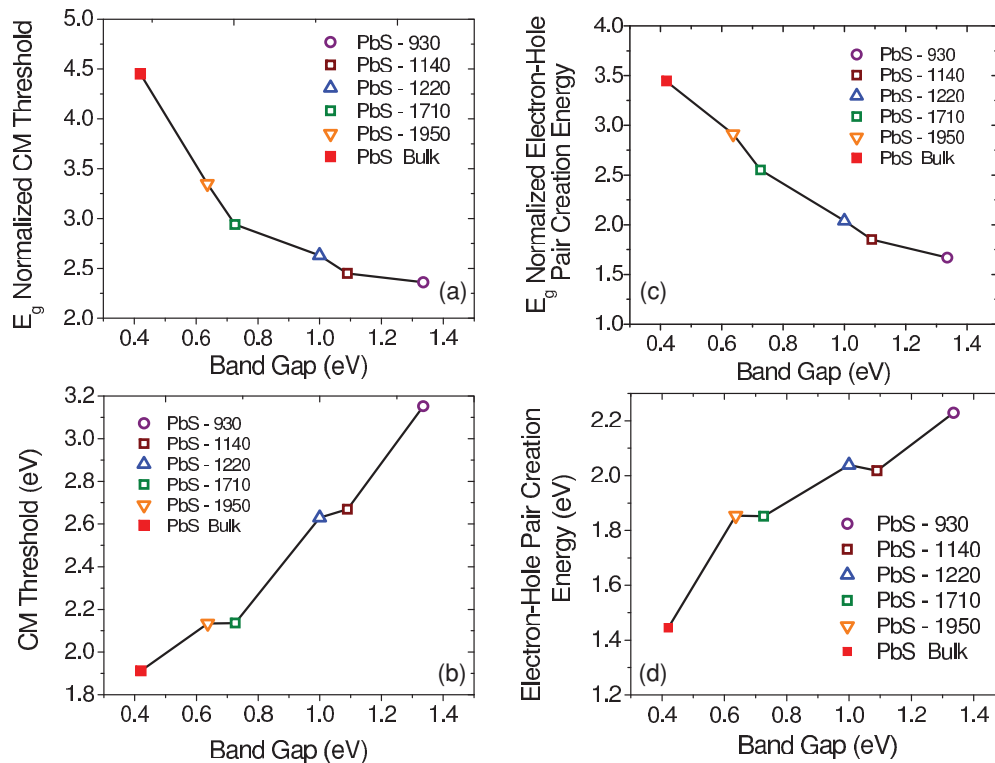


FIG. 4. (Color online) Carrier-multiplication energy threshold (a) normalized by the sample band gap and (b) in terms of absolute energy and electron-hole-pair creation energy (c) normalized by the sample band gap and (d) in terms of absolute energy plotted vs the sample band gap.

In addition, despite the fact that PbS is more symmetric and isotropic than PbSe, Kang and Wise<sup>36</sup> have shown, using a simple  $k\cdot p$  approximation, that PbS and PbSe QDs present very similar densities of states and intraband transition energies for the range of band gaps studied here.

While impact ionization is known to be the mechanism responsible for CM in bulk semiconductors, several authors have proposed different models to explain CM in semiconductor QDs.<sup>1,12,15</sup> Schaller *et al.*<sup>1</sup> have shown that CM happens on time scales shorter than 200 fs in PbSe QDs, therefore suggesting that direct photogeneration of multiexcitons via virtual single-exciton states should be considered to explain the observed dynamics. On the other hand, a recent report from Franceschetti *et al.*<sup>15</sup> predicts that, for PbSe, impact ionization in the case of electrons excited by photon energies larger than 3 eV can be as fast as 20 fs.

Pijpers *et al.*<sup>2</sup> use a tight-binding model to calculate the density of state of PbSe QDs and estimate the CM efficiency as a function of the photon energy for different sizes of PbSe QDs considering only impact ionization. The results show a decrease of the CM efficiency for smaller QDs, at a given photon energy. The enhanced Coulomb interaction in smaller QDs is expected to improve the CM in QDs,<sup>12</sup> however, the reduction of the QD sizes also decreases the density of states, which should lead to a decrease of the impact ionization.<sup>2</sup> In Fig. 5, we compare the calculations of CM for PbSe QDs with  $E_g = 0.6$  and 1.2 eV from Ref. 2 to our data for PbS QDs with similar band gaps. We find good qualitative agreement between our experimental results for PbS and the theoretical predictions for PbSe QDs of similar band gap. Both results indicate a blue shift of the CM energy threshold for smaller QDs and a decrease of  $\varepsilon$  (in  $\hbar\omega/E_g$ ) for QDs with larger band gap. This qualitative agreement could be explained by the similar density of states of both structures. However, we see that the experimental values of CM for PbS QDs are lower than those predicted for PbSe. A possible explanation for such a difference is the fact that the theoretical calculations shown in Fig. 5 are performed considering the same phonon-assisted decay lifetime (0.5 ps) for QDs of different sizes; however,

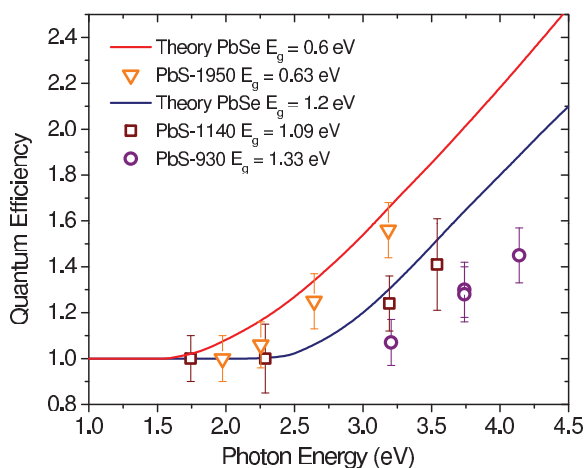


FIG. 5. (Color online) Comparison of experimental results for CM efficiency in PbS QDs to theoretical predictions of carrier multiplication via impact ionization for PbSe QDs with similar band gap from Ref. 2.

from the results of Figs. 1 and 2, we conclude that the intraband relaxation is faster in smaller QDs. Furthermore, the phonon-assisted cooling is expected to have a faster energy loss rate for higher excited electrons.<sup>1</sup> The phonon-assisted decay competes with CM as a cooling process for the high-energy electrons, and a decrease of the phonon-assisted decay lifetime would lead to less efficient CM.<sup>2,20</sup>

The good qualitative agreement between theory and experiment shown in Fig. 5 suggests that, as for bulk semiconductors, CM in QDs can be explained by impact ionization and that there is no need to invoke intermediate virtual levels to explain the CM threshold lower than  $3 E_g$  for lead-salt QDs.

### C. Comparison between static and flowing sample

The results shown in Fig. 3 are obtained mostly from pump-probe measurements performed in static QDs where no stirring or flow cell was used (the flow-cell test was not possible for some samples due to the large amount of sample required for this experiment). McGuire *et al.*<sup>13</sup> have shown that, for some PbSe QDs, significant differences in CM efficiency are observed between static and stirred QD samples under UV excitation ( $\hbar\omega > 3$  eV). The larger apparent CM efficiency in static samples has been attributed to cumulative photoionization of the QDs, which is expected to be long lived and highly dependent on both the pump photon energy and the sample investigated (properties such as the degree of surface passivation are expected to strongly influence the photoionization of QDs).<sup>13,37,38</sup> To investigate the influence of any long-lived process on our CM signals, we have performed two different tests: (1) We verified the absence of an increase in transmittance when the delay is set such that the probe precedes the pump pulse (negative time delay). The presence of long-lived photoionization (approximately tens of seconds as recently reported in Refs. 37 and 38) is expected to cumulatively decrease the linear absorption of the QDs, leading to increased transmittance of the probe beam due to the presence of the pump, even for negative time delays for the 1-kHz repetition rate of the excitation source. No measurable changes in the linear transmittance of the probe due to the presence of the pump were observed (even for large pump fluences,  $(N) \sim 1$  photon absorbed per QD), suggesting that, if there is photoionization in the samples investigated, the effect is small. (2) For the smallest QD samples, for which the CM was measured under excitation with photon energy greater than 3 eV, we performed comparative transient absorption studies of CM in static and flowing QD solutions. The flow cell (with cross-sectional area of 1 mm  $\times$  10 mm) was set to a flow rate of 600 ml/min, which is sufficient for the pumped and probed sample volume ( $\sim 10^{-3}$  ml) to be almost completely replaced in less than 1 ms (laser repetition rate of 1 kHz).<sup>38</sup> Considering the depletion of the pump beam due to the high optical density, mainly at photon energies higher than 3 eV ( $OD \sim 2.0$ ), and the flow dynamics, less than 10% of the QDs can be excited by more than one pump pulse. Figure 6 shows a comparison between the results obtained for the sample PbS-930 in the static and flow case (pump at 300 nm). For the static versus flowing study, no significant difference has been observed, indicating that if photoionization is influencing our CM results,

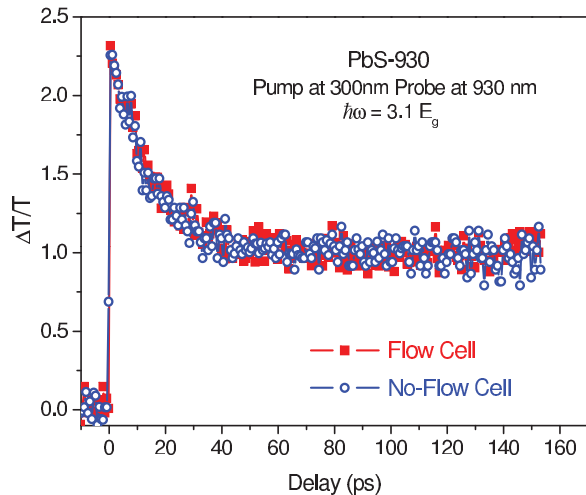


FIG. 6. (Color online) Comparison of pump and probe measurement for static and flowed suspension of PbS-930 at high pump fluence (average number of absorbed photons  $\sim 0.6$  per QD) and  $\hbar\omega = 3.1 E_g$ .

this phenomenon should not account for more than  $\sim 10\%$  of our CM signal, defined by the experimental noise from our results (Fig. 6). The result from the flow-cell experiment together with the other tests described above suggests that the influence of photoionization is minimal in our measurements.

McGuire *et al.*<sup>14</sup> have proposed a model to correct any apparent CM efficiency due to the presence of photoionization in up-converted photoluminescence<sup>39</sup> experiments, assuming that charging of the QDs does not change the CM efficiency. Following the assumptions from Ref. 14, for the case of low excitation (no more than 1 photon absorbed per QD) and a CM yield less than 100%, we calculate the true multiplication yield (CM yield free of the influence of photoionization as defined in Ref. 14) for transient absorption experiments under the presence of photoionization, obtaining

$$\eta = (1 + \eta_{\text{App}})(1 - f) - 1, \quad (1)$$

where  $\eta_{\text{App}}$  and  $\eta$  are the apparent and true multiplication yield<sup>14</sup> and  $f$  is the fraction of photocharged QDs. In Fig. 6, we see no difference (within the experimental noise of  $\sim 10\%$ ) between the signal at long delays for the static and flowing samples, indicating that less than 10% of the QDs are affected by photoionization. Assuming that, for the excitation at 4.1 eV, 10% of the QDs are influenced by photoionization, from Eq. (1), the real CM efficiency would be  $\sim 11\%$  lower than that measured. For the two largest QDs shown in Fig. 3, no CM experiments under flowing conditions were performed. However, for PbS-1710 and PbS-1950, most of the CM data were obtained with excitation photon energy below 3.0 eV, where no strong influence of photoionization is expected.<sup>37,38</sup> For these samples, the highest photon energy used for the pump was 3.18 eV, corresponding to the highest CM efficiency for the samples PbS-1710 and PbS-1950 in Fig. 3. Consequently, these points at 3.18 eV could be artificially high due to photoionization. A possible influence of photoionization in our CM measurements could only slightly change the electron-hole-pair creation energy and the CM threshold in our

measurements. Therefore, the possible influence of the photoionization does not change our qualitative conclusions that the CM efficiency decreases for smaller QDs at a given photon energy and, if compared in terms of relative energy ( $\hbar\omega/E_g$ ), both the CM energy threshold and  $\varepsilon$  decrease with stronger quantum confinement.

## II. CONCLUSIONS

Our study of carrier dynamics and carrier multiplication in several sizes of PbS quantum dots reveals that the intraband dynamics follows the same trend previously observed in PbSe (Ref. 21) and CdSe (Ref. 22) QDs, which suggests the absence of a phonon bottleneck, i.e., the intraband  $1P \rightarrow 1S$  decay is faster for smaller QDs, ranging from  $\sim 300$  to  $\sim 3$  ps. The eight-fold degeneracy of the  $1S$  level is observed from the saturation of the bleaching of the  $1S_h \rightarrow 1S_e$  peak, and a long-lived decay is observed from the  $1P$  level if this level is initially populated by more than eight carriers.

The study of the size dependence of CM in PbS QDs reveals that the threshold for CM is nearly constant at  $\sim 2.0$ – $2.1$  eV, but the quantum confinement leads to a blue shift of the CM threshold for PbS QDs with  $E_g > 1$  eV. In addition, the results show that the energy efficiency of CM in QDs is larger than in bulk PbS and, in terms of band gap, the CM threshold energy approaches  $2.35 E_g$ , which agrees with predictions from impact-ionization models.<sup>2,19</sup> Equally, the electron-hole-pair creation energy is reduced from  $3.4 E_g$  for bulk PbS to  $1.7 E_g$  for the smallest QDs. In other words, the enhanced Coulomb interaction in smaller QDs is compensated by the decrease of the density of states leading to the decrease of the CM efficiency at a given photon energy for smaller QDs;<sup>2</sup> however, for the same ratio of  $\hbar\omega/E_g$ , the CM is enhanced in smaller QDs, ultimately getting closer to the energy conservation limit. This also leads to higher electron-hole-pair multiplication efficiency. As shown by Beard *et al.*, these trends can be advantageous in photovoltaic devices.<sup>12</sup>

The spectral behavior of the CM for PbS QDs agrees well with theoretical predictions of impact ionization for PbSe QDs with the same band gap, confirming the prediction by Lou *et al.*<sup>18</sup> that the degeneracy of the band-edge states (eight-fold degenerate  $1S$  level for both PbS and PbSe) and the density of states are the important factors defining the efficiency of impact ionization in semiconductors. This also suggests that no additional processes are required to explain CM in these quantum-confined materials, and, as in the bulk semiconductor, the CM is due to impact ionization. The amount of QD photocharging was also investigated, showing no measurable influence on our results.

## ACKNOWLEDGMENT

This material is based upon work supported in part by the U.S. Army Research Office under Contract/Grant No. 50372-CH-MUR, the Air Force Office of Sponsored Research MURI AFOSR Grant No. FA9550-06-1-0337, the DARPA ZOE program Grant No. W31R4Q-09-1-0012, and the Israel Ministry of Defense Contract No. 993/54250-01.

\*hagan@creol.ucf.edu

†ewvs@creol.ucf.edu

- <sup>1</sup>R. D. Schaller, V. M. Agranovich, and V. I. Klimov, *Nat. Phys.* **1**, 189 (2005).
- <sup>2</sup>J. J. H. Pijpers, R. Ulbricht, K. J. Tielrooij, A. Osherov, Y. Golan, C. Delerue, G. Allan, and M. Bonn, *Nat. Phys.* **5**, 811 (2009).
- <sup>3</sup>P. T. Landsberg, *Recombination in Semiconductors* (Cambridge University, Cambridge, UK, 1991).
- <sup>4</sup>V. Sukhovatkin, S. Hinds, L. Brzozowski, and E. H. Sargent, *Science* **324**, 1542 (2009).
- <sup>5</sup>V. I. Klimov, *Appl. Phys. Lett.* **89**, 123118 (2006).
- <sup>6</sup>M. C. Beard, A. G. Midgett, M. C. Hanna, J. M. Luther, B. K. Hughes, and A. J. Nozik, *Nano Lett.* **10**, 3019 (2010).
- <sup>7</sup>V. I. Rupasov and V. I. Klimov, *Phys. Rev. B* **76**, 125321 (2007).
- <sup>8</sup>R. D. Schaller, M. Sykora, J. M. Pietryga, and V. I. Klimov, *Nano Lett.* **6**, 424 (2006).
- <sup>9</sup>R. J. Ellingson, M. C. Beard, J. C. Johnson, P. Yu, O. I. Micic, A. J. Nozik, A. Shabaev, and A. L. Efros, *Nano Lett.* **5**, 865 (2005).
- <sup>10</sup>R. D. Schaller, J. M. Pietryga, and V. I. Klimov, *Nano Lett.* **7**, 3469 (2007).
- <sup>11</sup>R. D. Schaller, M. A. Petruska, and V. I. Klimov, *Appl. Phys. Lett.* **87**, 253102 (2005).
- <sup>12</sup>M. C. Beard, K. P. Knutsen, P. Yu, J. M. Luther, Q. Song, W. K. Metzger, R. J. Ellingson, and A. J. Nozik, *Nano Lett.* **7**, 2506 (2007).
- <sup>13</sup>J. A. McGuire, J. Joo, J. F. Pietryga, R. D. Schaller, and V. I. Klimov, *Acc. Chem. Res.* **41**, 1810 (2008).
- <sup>14</sup>J. A. McGuire, M. Sykora, J. Joo, J. M. Pietryga, and V. I. Klimov, *Nano Lett.* **10**, 2049 (2010).
- <sup>15</sup>A. Franceschetti, J. M. An, and A. Zunger, *Nano Lett.* **6**, 2191 (2006).
- <sup>16</sup>G. Nair, S. M. Geyer, L. Y. Chang, and M. G. Bawendi, *Phys. Rev. B* **78**, 125325 (2008).
- <sup>17</sup>L. Silvestri and V. M. Agranovich, *Phys. Rev. B* **81**, 205302 (2010).
- <sup>18</sup>J. W. Luo, A. Franceschetti, and A. Zunger, *Nano Lett.* **8**, 3174 (2008).
- <sup>19</sup>C. Delerue, G. Allan, J. J. H. Pijpers, and M. Bonn, *Phys. Rev. B* **81**, 125306 (2010).
- <sup>20</sup>G. Allan and C. Delerue, *Phys. Rev. B* **73**, 205423 (2006).
- <sup>21</sup>R. D. Schaller, J. M. Pietryga, S. V. Goupalov, M. A. Petruska, S. A. Ivanov, and V. I. Klimov, *Phys. Rev. Lett.* **95**, 196401 (2005).
- <sup>22</sup>V. I. Klimov and D. W. McBranch, *Phys. Rev. Lett.* **80**, 4028 (1998).
- <sup>23</sup>E. H. Sargent, *Adv. Mater. (Weinheim, Ger.)* **17**, 515 (2005).
- <sup>24</sup>M. A. Hines and G. D. Scholes, *Adv. Mater. (Weinheim, Ger.)* **15**, 1844 (2003).
- <sup>25</sup>L. Cademartiri, E. Montanari, G. Calestani, A. Migliori, A. Guagliardi, and G. A. Ozin, *J. Am. Chem. Soc.* **128**, 10337 (2006).
- <sup>26</sup>R. A. Negres, J. M. Hales, A. Kobayakov, D. J. Hagan, and E. W. Van Stryland, *IEEE J. Quantum Electron.* **38**, 1205 (2002).
- <sup>27</sup>V. I. Klimov, *Annu. Rev. Phys. Chem.* **58**, 635 (2007).
- <sup>28</sup>M. T. Trinh, A. J. Houtepen, J. M. Schins, J. Piris, and L. D. A. Siebbeles, *Nano Lett.* **8**, 2112 (2008).
- <sup>29</sup>G. Nootz, L. A. Padilha, P. D. Olszak, S. Webster, D. J. Hagan, E. W. Van Stryland, L. Levina, V. Sukhovatkin, L. Brzozowski, and E. H. Sargent, *Nano Lett.* **10**, 3577 (2010).
- <sup>30</sup>J. Seebeck, T. R. Nielsen, P. Gartner, and F. Jahnke, *Phys. Rev. B* **71**, 125327 (2005).
- <sup>31</sup>T. Inoshita and H. Sakaki, *Phys. Rev. B* **46**, 7260 (1992).
- <sup>32</sup>E. Istrate, S. Hoogland, V. Sukhovatkin, L. Levina, S. Myrskog, P. W. E. Smith, and E. H. Sargent, *J. Phys. Chem. B* **112**, 2757 (2008).
- <sup>33</sup>A. Pandey and P. Guyot-Sionnest, *J. Phys. Chem. Lett.* **1**, 45 (2010).
- <sup>34</sup>J. M. Caruge, Y. Chan, V. Sundar, H. J. Eisler, and M. G. Bawendi, *Phys. Rev. B* **70**, 085316 (2004).
- <sup>35</sup>J. B. Sambur, T. Novet, and B. A. Parkinson, *Science* **330**, 63 (2010).
- <sup>36</sup>I. Kang and F. W. Wise, *J. Opt. Soc. Am. B* **14**, 1632 (1997).
- <sup>37</sup>J. A. McGuire, M. Sykora, I. Robel, L. A. Padilha, J. Joo, J. M. Pietryga, and V. I. Klimov, *ACS Nano* **4**, 6087 (2010).
- <sup>38</sup>A. G. Midgett, H. W. Hillhouse, B. K. Hughes, A. J. Nozik, and M. C. Beard, *J. Phys. Chem. C* **114**, 17486 (2010).
- <sup>39</sup>J. Shah, *IEEE J. Quantum Electron.* **24**, 276 (1988).